

CO Emission in Low Luminosity, HI Rich Galaxies

Christopher L. Taylor

Ruhr-Universität Bochum, Astronomisches Institut
Universitätsstr 150, D-44870 Bochum
Germany

Henry A. Kobulnicky¹

University of California, Santa Cruz
Lick Observatory/Board of Studies in Astronomy
Santa Cruz, CA, 95064

Evan D. Skillman

University of Minnesota, Department of Astronomy
116 Church St. SE
Minneapolis, MN 55455

Received _____; accepted _____

¹Hubble Fellow

ABSTRACT

We present ^{12}CO $1 \rightarrow 0$ observations of eleven low luminosity ($M_B > -18$), HI-rich dwarf galaxies. Only the three most metal-rich galaxies, with $12+\log(\text{O/H}) \approx 8.2$, are detected. Very deep CO spectra of six extremely metal-poor systems ($12+\log(\text{O/H}) \leq 7.5$) yield only low upper limits on the CO surface brightness, $I_{CO} < 0.1 \text{ K km s}^{-1}$. Three of these six have never before been observed in a CO line, while the others now have much more stringent upper limits. For the very low metallicity galaxy Leo A, we do not confirm a previously reported detection in CO, and the limits are consistent with another recent nondetection.

We combine these new observations with data from the literature to form a sample of dwarf galaxies which all have CO observations and measured oxygen abundances. No known galaxies with $12+\log(\text{O/H}) < 7.9$ ($Z < 0.1Z_\odot$) have been detected in CO. Most of the star-forming galaxies with higher ($12+\log(\text{O/H}) > 8.1$) metallicities are detected at similar or higher I_{CO} surface brightnesses. The data are consistent with a strong dependence of the $I_{CO}/M_{H_2} \equiv X_{CO}$ conversion factor on ambient metallicity. The strikingly low upper limits on some metal-poor galaxies lead us to predict that the conversion factor is non-linear, increasing sharply below $\sim 1/10$ of the solar metallicity ($12+\log(\text{O/H}) \leq 7.9$).

Subject headings: galaxies: dwarf — galaxies: ISM

1. Introduction

Carbon monoxide (CO) is commonly used as a tracer of cool molecular gas, because molecular hydrogen (H_2), the dominant species in the molecular phase, has no strong emission lines from which the column density of H_2 may easily be determined. Since the rotational transitions of CO in the millimeter and submillimeter regime are relatively easy to excite, it is possible to use the luminosity in one of these lines to estimate the column density and mass of molecular gas, provided one knows the correct conversion. The conversion factor, X_{CO} , from I_{CO} to N_{H_2} has been determined for the Milky Way galaxy to be $\sim 3 \times 10^{20} \text{ cm}^{-2} (\text{K km s}^{-1})^{-1}$ for the $^{12}\text{CO} 1 \rightarrow 0$ transition (Strong et al. 1988; Scoville & Sanders 1987). The application of this Milky Way value to external galaxies has been controversial, as the value may depend on the physical conditions in those galaxies which are difficult to determine observationally and may differ greatly from those in our own galaxy (Dickman, Snell & Schloerb 1986; Israel et al. 1986; Maloney & Black 1988, hereafter MB88).

One of the characteristics of a galaxy which may affect the relation between CO luminosity and H_2 gas mass is its metal abundance. If the abundance of the CO molecule is low, the column density of CO may not be great enough to allow self shielding from dissociating radiation. In this case, the size of the CO emitting region within a given molecular cloud will shrink, while the H_2 is unaffected. Thus the filling factor will decrease, reducing the CO luminosity for a given molecular gas mass (MB88). Rubio, Lequeux & Boulanger (1993) have found observational evidence of this effect in the SMC. Their data for a number of molecular clouds show a correlation between cloud size and the CO-to- H_2 conversion factor. They suggest that the smaller clouds are the dense cores of larger clouds in which the diffuse CO outside the cores has been dissociated (cf. MB88).

Observational studies have led to conflicting conclusions concerning the presence of

molecular clouds in actively star forming dwarf galaxies. Since the pioneering work of Elmegreen, Elmegreen, & Morris (1980), it has been clear that the CO molecule is difficult to detect in dIs and therefore, that the CO surface brightnesses are much lower in dIs than in spiral galaxies. Under the assumption that the CO/H₂ ratio is constant everywhere, this implied that the molecular gas content of dwarf galaxies must be very low (Young, Gallagher, & Hunter 1984; Tacconi & Young 1987).

On the other hand, studies by Wilson (1995, hereafter W95) and Verter & Hodge (1995) have provided strong evidence that the conversion factor depends on the metal abundance of the galaxy. By measuring molecular cloud virial masses and comparing them to their CO luminosities, W95 showed that the CO-to-H₂ conversion increases as the metallicity of the host galaxy decreases over the range of $8 \leq 12 + \log(\text{O/H}) \leq 9$. This supported the conclusions made by Cohen et al. (1988) and Rubio et al. (1991) based on observations of the Magellanic Clouds. Verter & Hodge (1995) added very deep CO 2 → 1 observations of the extreme dwarf galaxy GR 8 and were unable to detect any CO. The proximity of GR 8 (2.2 Mpc, Tolstoy et al. 1995) allows very low upper limits on L(CO). Combined with an inference of the minimal molecular mass present to support the current star formation in GR 8, this was also interpreted as an indication of a metallicity dependence of the CO-to-H₂ conversion factor.

Studies of this type have been limited primarily to galaxies of relatively high metallicities in order to detect CO emission. Indeed, the non-detection of GR 8 by Verter & Hodge (1995), with an oxygen abundance of $12 + \log(\text{O/H}) = 7.47$ (Skillman, Kennicutt & Hodge 1989) illustrates this difficulty. In fact, the only low metallicity dwarf irregular galaxy to have been detected in CO is Leo A, observed by Tacconi & Young (1987), at $12 + \log(\text{O/H}) = 7.3$. A recent observation of Leo A by L. Young (Young 1997, private communication) failed to confirm the detection of CO in Leo A. We decided to try to

confirm this important result ourselves, and to supplement the understanding of CO emission in low metallicity environments by observing additional metal poor dwarf galaxies.

Here we present ^{12}CO $1 \rightarrow 0$ observations of 11 galaxies covering a range of oxygen abundances from $7.3 \geq 12+\log(\text{O/H}) \geq 8.2$. Some of these galaxies have been previously observed in CO. We confirm previous detections for several galaxies, and we obtain very deep upper limits for others. We present the first published CO data on three galaxies, UGC 4483, DDO 187 and UM422. Section 2 contains a description of the observations and data reduction while Section 3 describes the results. In Section 4 we combine the new observations with a thorough search of the literature to examine the relationship between CO surface brightness and metal abundance in these low-mass systems.

2. ^{12}CO Observations and Data Reduction

2.1. Observations

We observed 5 galaxies with the NRAO² 12-m telescope at Kitt Peak, in the $1 \rightarrow 0$ (115 GHz) transition of ^{12}CO on 5 – 11 January 1998: Leo A, Sextans A, DDO 210, DDO 187, and Pegasus. Three galaxies (UM422, Mrk 178 and UGC 4483) were observed on 10–13 March 1994 and 3 more (NGC 1569, NGC4214, and NGC5253) on 18–21 June 1995. The 3 mm SIS receiver was used with the filterbank spectrometer and a 1 MHz filter, yielding 256 channels per spectrum, and a channel width of 2.6 km s^{-1} . The receiver was tuned to the central velocity of the HI distribution in each galaxy. Operating at 115 GHz, the half power beam width is $55''$. System temperatures varied from between ~ 300 K to 500 K during the course of the observations, infrequently rising higher during the January 1998 run due to

²The National Radio Astronomy Observatory is a facility of the National Science Foundation, operated under cooperative agreement by Associated Universities, Inc.

weather conditions. The pointing was checked about every two hours by observing Venus or Mars. The observations were conducted in beam switching mode, with a beam throw of $2'$ at 1.25 Hz, except for Leo A and Sextans A which have too large an angular extent. For these galaxies, the absolute position switching mode was used to ensure a reference beam uncontaminated by emission from the galaxy. For comparison, one position in Leo A was also observed in beam switching mode.

2.2. Observing Strategy

Part of the motivation for our observations was to re-observe Leo A to confirm the detection of Tacconi & Young (1987). Since those original observations, HI interferometer maps for a number of dwarf galaxies, including Leo A, have become available. In particular, Young & Lo (1996) obtained VLA HI observations of Leo A at high spatial and velocity resolution. They discovered a new, cold component to the atomic gas, with a velocity dispersion $\sigma \simeq 3.5 \text{ km s}^{-1}$, in addition to the well known warm component with $\sigma \simeq 9 \text{ km s}^{-1}$. We reasoned that this cold component of the HI was the most likely area to find CO emission in these galaxies, if it was detectable. As this cold HI gas is found at the regions of highest HI column density, we used interferometer maps to direct our CO observations for Leo A, Sextans A, DDO 210, DDO 187 and Pegasus. For the other galaxies we pointed at the center of the stellar distributions, except for NGC 4214, which we observed at 4 positions within the galaxy.

2.3. Data Reduction

From each individual scan we subtracted a linear baseline and averaged multiple scans weighted by a factor of $1/T_{sys}^2$. We rejected scans showing unstable baselines which could

not be fit with a linear baseline. The resulting averaged spectra for the galaxies with the smallest velocity widths (Leo A, Sextans A, DDO 210, DDO 187, and Pegasus) are smoothed to 5.2, 10.4 and 20.8 km s^{-1} resolution. The remaining galaxies with broader HI line widths we smoothed to 20.8 km s^{-1} . Total integration times for each object ranged between 6 and 8 hours, including 50% of the time spent on the sky reference position. We searched spectra at each resolution for ^{12}CO $1 \rightarrow 0$ emission. Original resolution and smoothed spectra for each galaxy appear in Figure 1. A horizontal bar indicates the width of the HI profile. Temperatures indicate brightness units on the T_R^* scale.

EDITOR: PLACE FIGURE 1 HERE.

3. Results: CO Detections and Upper Limits

3.1. Individual Galaxies

Table 1 gives the positions, optical diameters, HI heliocentric central velocities and velocity widths from the literature for each of the newly observed galaxies, as well as the central velocities, velocity widths (full widths at 50% max), the rms noise and the integrated intensities ($I_{CO} = \int T_R^* dv$) of the CO line or the upper limits. Reported errors on I_{CO} are computed from $\sqrt{N} \times \sigma_{rms} \times \delta v_{chan}$ where N is the number of channels where CO was detected, σ_{rms} is the noise in the spectrum, and δv_{chan} is the channel width in km s^{-1} .

EDITOR: PLACE TABLE ?? HERE.

Leo A— Leo A is a dwarf irregular galaxy for which Tacconi & Young (1987) claim a CO detection. We observed three positions in this galaxy, two corresponding to the locations of the cold HI component discovered by Young & Lo (1996), and the third at the

same position observed by Tacconi & Young (1987). Comparing this position with the HI map of Young & Lo (1996) shows that the claimed CO detection arises in a large depression in the HI column density. We detected CO at *none* of the three positions, including that observed by Tacconi & Young. The non-detection of CO is in accord with the low metallicity of Leo A and the non-detection of other systems with similarly low metallicities. The rms noise for the spectra we have obtained in Leo A range from 2.7 to 5.5 mK when smoothed to 5.2 km s^{-1} velocity resolution. For a resolution of 20.8 km s^{-1} the range is 1.3 to 2.6 mK. In comparison, the detection from Tacconi & Young is 19 mK with a velocity width of 25 km s^{-1} .

Sextans A— The dwarf irregular galaxy Sextans A was most recently observed in CO (prior to our own observations) by Ohta et al. (1993). They observed a single position coinciding with the peak HI column density determined from the map of Skillman et al. (1988), attaining an rms noise in their spectrum of 48 mK for a velocity resolution of 2.6 km s^{-1} . We have observed two positions in Sextans A, the main peak in the HI column density, as well as a secondary peak. These two peaks are positioned on either side of a depression in the HI column density that coincides with the center of the optical galaxy. In our observations of the secondary HI peak (labeled as position 3 in Table 1) we used the the HI hole as the position for the reference beam. Thus emission at that location would appear as an absorption feature in the spectrum of Figure 1. The velocity difference between the gas at these two locations due to the rotation of the galaxy is large enough ($\sim 10 \text{ km s}^{-1}$) that an apparent absorption feature would not cancel out emission at position 3. The rms noise in our spectra span the range 3.4 to 5.5 mK at 5.2 km s^{-1} velocity resolution, and 1.3 to 2.4 mK for 20.8 km s^{-1} resolution.

DDO 210— DDO 210, another gas rich dwarf irregular galaxy, is among those observed in CO by Tacconi & Young (1987), who did not detect it. They give a 2σ upper limit on the

integrated CO intensity, I_{CO} of 0.41 K km s^{-1} , compared to our 5σ upper limit of 0.12 K km s^{-1} . We used the HI maps by Lo, Sargent, & Young (1993) to direct our single pointing observation at the peak of the HI column density. The Tacconi & Young (1987) position falls approximately one beam width to the east of ours, although still on an area of high HI column density. We note that the oxygen abundance we use for DDO 210 is derived from its absolute magnitude using the luminosity–metallicity relation of Skillman, Kennicutt & Hodge (1989). This is necessary because it does not have HII regions in which oxygen lines can be observed (van Zee, Haynes & Salzer 1997).

DDO 187— DDO 187 is also a dwarf irregular, but it has not been previously observed in CO. We obtained a spectrum from a single position in the galaxy, centered on the peak of the HI column density as determined from the data of Lo, Sargent, & Young (1993). Smoothing the spectrum to 5.2 km s^{-1} , we reach an rms noise of 2.7 mK , while for 20.8 km s^{-1} the noise is 1.6 mK .

Pegasus— The Pegasus dwarf irregular galaxy has also been observed in CO by Tacconi & Young (1987), who do not detect it, giving a 2σ upper limit on the integrated CO intensity of 0.38 K km s^{-1} . This compares to our 5σ upper limit of $0.080 \text{ K km s}^{-1}$. The position observed by Tacconi & Young (1987) is $\sim 1'$ north of the position we have observed, and is on the edge of the dense region of HI for which our observed position is the HI peak.

NGC 5253— The amorphous galaxy NGC 5253 is a 4σ detection in the smoothed spectrum, with a peak intensity at roughly 400 km s^{-1} , the systemic velocity of the HI distribution. Turner, Beck & Hurt (1997) also obtained a detection ($14 \text{ Jy km s}^{-1} = 6 - 8\sigma$) of NGC 5253 at the velocity of the HI using the Owens Valley Radio Observatory millimeter array. Using the SEST telescope, Wiklind & Henkel (1989) find an integrated CO intensity of 1.3 K km s^{-1} , which corresponds to $27.3 \text{ Jy km s}^{-1}$ assuming a gain of 21

Jy/K at 115 GHz. For the 12 m telescope, we adopt a gain of 34 Jy/K (NRAO 12m user's guide) which yields 24.6 ± 5.0 Jy km s^{-1} , consistent with the SEST value, and roughly twice the OVRO interferometer value. The discrepancy between single dish and interferometer measurements is to be expected if the interferometer resolves out CO emission on large angular scales. NGC 5253 was also observed by Jackson et al. (1989), who did not detect it with the NRAO 12-m telescope, with an rms noise of 0.10 K in their spectrum, a value slightly higher than in our own spectrum.

NGC 1569— NGC 1569 has been classified as a Magellanic irregular. Israel & de Bruyn (1988) have found evidence that it is in a post starburst phase, in which the massive star formation has recently ceased. For this galaxy we find an integrated CO intensity of 0.685 ± 0.104 K km s^{-1} . The CO spectrum shows an absorption signature near 0 km s^{-1} due to Galactic foreground CO emission in the reference beam. Rogstad et al. (1967) obtained an HI spectrum towards NGC 1569 which shows HI emission at $\sim -90 \text{ km s}^{-1}$, and also detected a narrow emission feature at $\sim 0 \text{ km s}^{-1}$ from the Galaxy. The two features are well separated so there should not be any contamination from the off-beam reference position affecting the line profile. Israel Tacconi, & Baas (1995) obtained an upper limit with a peak T_R^* of 0.024 K. Young, Gallagher, & Hunter (1984) detected NGC 1569 at $I_{CO} = 1.6 \pm 0.3$ K km s^{-1} , more than twice our detected level. We do not know the reason for this difference, but we note that the Israel et al. (1995) value is consistent with our measurement and inconsistent with Young et al. (1984). Greve et al. (1996) have mapped the CO distribution in NGC 1569 in both the $1 \rightarrow 0$ and $2 \rightarrow 1$ lines. In these maps, the CO emission is confined to an area approximately $20'' \times 20''$, small enough to be contained in our $55''$ beam.

NGC 4214— NGC 4214 is classified as SBmIII and is one of the most luminous of the observed galaxies. Four positions separated by $45''$, were observed. These are designated

a,b,d and e. CO is detected at 2 of the 4 positions, with an integrated CO intensity of $0.900 \pm 0.105 \text{ K km s}^{-1}$. A direct comparison of these results to other CO observations of NGC 4214 is problematic because of different beam sizes (IRAM; Becker et al. 1995) or overlapping beams (Thronson et al. 1988). Our results are at least consistent with the center position 3σ detections reported by Thronson et al. ($I_{CO} = 1.0 \pm 0.35 \text{ K km s}^{-1}$) and Tacconi & Young (1985; $I_{CO} = 0.94 \pm 0.22 \text{ K km s}^{-1}$). Becker et al. (1995) have mapped this galaxy in the ^{12}CO $2 \rightarrow 1$ transition, finding the emission to be confined to a region roughly thirty arcseconds in diameter. Our observations cover this area and should detect all the ^{12}CO $1 \rightarrow 0$ emission.

Mrk 178— Mrk 178 is a low luminosity dwarf with an abundance of $12 + \log(\text{O/H}) = 8.0$ (Kobulnicky & Skillman, in prep.) Mrk 178 has been observed in CO previously, but has only a high upper limit (rms noise = 20 mK, Morris & Lo 1978). Our spectrum shows no emission down to a limit of $I_{CO} < 0.2 \text{ K km s}^{-1}$. The rms noise in the final averaged spectra is 2 mK, a factor of 10 lower than that obtained by Morris & Lo (1978).

UGC 4483— UGC 4483 is a very low abundance dwarf galaxy ($12 + \log(\text{O/H}) = 7.5$) in the nearby M81 group (Skillman et al. 1994). Its appearance is dominated by a single giant star forming complex. It has no previous CO observations in the literature, and no CO emission was detected in our spectrum, which has an rms noise of 2 mK. The upper limit on I_{CO} is $< 0.195 \text{ K km s}^{-1}$.

UM422— The HII galaxy UM422 (UGC 6345) is an emission line galaxy from the sample of Salzer, MacAlpine, & Boroson (1989), and was included in the VLA HI survey of HII galaxies of Taylor et al. (1995). It is the most distant galaxy in this paper, and was included in our sample because of its low metal abundance. This galaxy has not been previous observed in CO. The rms noise in our spectrum is 2 mK, with an upper limit on I_{CO} of $0.120 \text{ K km s}^{-1}$.

Table 2 gives distances, optical luminosities, oxygen abundances, integrated CO intensities and CO “luminosities” for galaxies we have observed. L_{CO} is determined using the relation: $L_{CO} = I_{CO} A_S$, where A_S is the source area (e.g., Sanders, Scoville & Soifer 1991).

In the case of UM422, the most distant galaxy we observed, the star forming region traced by $H\alpha$ emission is approximately the size of the telescope beam. Thus this assumption of extended emission is adequate, as long as spatially extended star formation can be taken as indicating the presence of spatially extended molecular gas. Without a knowledge of the true CO spatial distribution, our assumption will at least provide reasonable *relative* estimates for the CO luminosities and H_2 masses among galaxies in our sample.

EDITOR: PLACE TABLE ?? HERE.

4. Discussion

4.1. The Dependence of CO Emission on Metal Abundance

We have carried out these observations with the goal of better understanding the relationship of CO emission to metal abundance in dwarf galaxies. Because all of these galaxies (with the exception of DDO 210) are currently experiencing at least some massive star formation, we can infer the presence of molecular gas. Even dwarf irregular galaxies with relatively low rates of massive star formation can be detected in CO, especially if they are nearby. To supplement our eleven galaxies we have searched the literature for low luminosity dwarfs which have been observed in the ^{12}CO $1 \rightarrow 0$ line. These previous works include Morris & Lo (1978), Rowan-Robinson, Phillips & White (1980), Elmegreen,

Elmegreen & Morris (1980), Israel & Burton (1986), Tacconi & Young (1987), Thronson & Bally (1987), Arnault et al. (1988), Sage et al. (1992), Wilson (1992), Hunter & Sage (1993), Brinks & Taylor (1995), Israel, Tacconi & Baas(1995), Young et al. (1995) and Gondhalekar et al. (1998). In an effort to keep the galaxy sample as homogeneous as possible, we selected only those galaxies with $M_B \geq -18$. For CO data, we are careful to convert I_{CO} from the published temperature units (usually T_{A*} or T_{mb}) into the units used here, T_{R*} . Since most galaxies have not been mapped in CO with an interferometer, we use the telescope beam size at the distance of the galaxy as a consistent first order estimate the source diameter. The data we have collected from the literature are presented in Table 3. Unfortunately, only a small fraction of these galaxies have published chemical abundances from optical spectroscopy.

EDITOR: PLACE TABLE ?? HERE.

Our primary objective is to study the dependence of CO emission on ambient metal abundance, independent of variations in galaxy size, distance, and optical luminosity. Verter & Hodge (1995) and Wilson (1995) use observations of individual molecular clouds in nearby galaxies to characterize the variation of X_{CO} with metallicity. Our data do not allow us to determine this conversion factor. Instead, our approach is to study a larger sample of extremely metal-poor galaxies using very sensitive CO observations obtained with a telescope beam that is comparable to the size of the target galaxies. Since the galaxies lie at different distances up to 20 Mpc, the telescope beam samples an ensemble average of many molecular clouds in the target galaxies. In most cases, the size of the CO emitting region is not known. Thus, the spectra for each pointing represent a mean CO surface brightness for the nearby resolved galaxies, and a lower limit on the CO surface brightness for the most distant objects where the emitting region may be much smaller than the beam. It is not immediately apparent which physical properties (e.g., I_{CO} , L_{CO} , M_{H_2}) derived from

the spectra make for the best analysis.

We first examined the CO luminosity, L_{CO} , as a function of metal abundance as indicated by $12 + \log(O/H)$. However, because metallicity correlates strongly with optical luminosity in galaxies of all types (e.g., Lequeux et al. 1979; Skillman, Kennicutt, & Hodge 1989) we find that more metal rich, and thus the most luminous, galaxies have larger L_{CO} . This result is not especially informative. Larger galaxies contain more matter, and not surprisingly, they should have more CO as well, even if the I_{CO}/N_{H_2} conversion factor is identical to smaller, more metal-poor galaxies. Next, we considered normalizing the CO luminosity of each galaxy by some fiducial indicator of its mass, such as optical luminosity or HI mass. This has the advantage of producing distance-independent quantities like L_{CO}/M_{HI} or L_{CO}/L_B . However, we find that for a given metal abundance, the scatter in each of these exceeds an order of magnitude. This scatter results, in part, because the CO, HI and optical data sample different regions of the galaxy. The HI and optical measurements refer to the global properties of a galaxy, including material at large radii, while, in all but the most distant targets, the CO data represent relatively localized measurements which cover only the central starforming regions. Furthermore, extinction and the recent star formation history strongly influences the measured optical luminosity. Ideally, such a normalization by optical luminosity or HI mass should be made using optical imaging or aperture synthesis HI mapping which is spatially matched to the single-dish CO beam.

We finally decided to use the integrated CO intensity, I_{CO} , as the unit of comparison between galaxies of different metallicity. I_{CO} is a measure of the mean CO surface brightness ($K \text{ km s}^{-1} \text{beam}^{-1}$), and is roughly independent of distance as long as the CO beam is not much larger than the emitting region. Since I_{CO} measures the amount of CO emission per unit beam area, the major problem with this quantity is that the CO beam subtends

larger areas with increasing galaxy distance. For more distant galaxies which are smaller than the beam area, the measured quantity represents only a lower limit on the CO surface brightness. In an effort to make a robust comparison between galaxies, we exclude from further analysis all objects more distant than 10 Mpc. At 10 Mpc, the 55" FWHM beam of the NRAO 12m telescope used in most of these observations subtends 2.7 kpc. This is approximately the size of CO emitting central regions of Magellanic irregular galaxies such as NGC 4214 (Becker et al. 1995). CO detections with 55" resolution in dwarf galaxies significantly more distant than 10 Mpc will yield probable lower limits on the CO surface brightness, I_{CO} . The opposite problem exists for very nearby galaxies where the telescope beam resolves individual giant molecular clouds. The CO data of Israel et al. (1993) in the LMC and SMC show a larger scatter in I_{CO} which probably reflects the real brightness variations between molecular clouds centers and inter-cloud regions. We include the LMC in the plot for comparison purposes, although it violates our absolute magnitude limit. For the LMC and SMC we adopt the mean I_{CO} values. Since Israel et al. (1993) chose locations in the LMC and SMC to contain molecular clouds and star-forming regions, this mean represents an upper limit on the true mean I_{CO} that would be observed from a distance of 2-5 Mpc which is typical of the dwarf galaxies under consideration. The rest of the galaxies in the sample (except NGC 6822) are more distant than 1 Mpc, so that these smaller scale brightness variations are smoothed out by the relatively larger beam area.

In Figure 2 we plot $\log I_{CO}$ versus the oxygen abundance ($12 + \log (O/H)$) for dwarf galaxies less than 10 Mpc away. Galaxies with CO detections appear as filled circles, while undetected objects appear as upper limits. We plot I Zw 36 with an open circle since it represents a less secure (4σ) detection (Tacconi & Young 1987; Young et al. 1995) and it has not been subsequently re-observed. We show only the brightest position for NGC 6822 reported by Wilson (1992). We plot the mean I_{CO} for the LMC and SMC reported by Israel et al. (1993).

Figure 2 reveals a clear dichotomy between systems with $12 + \log(\text{O/H}) > 8.0$ and the very metal-poor systems. All of the galaxies with CO detections have higher metallicities; the only one detected below $12 + \log(\text{O/H}) = 8.0$ is I Zw 36 (Tacconi & Young 1987). All galaxies with lower metallicities are non-detections with very low limits. The non-detections at low metallicities are consistent with a strong dependence of the CO surface brightness on metallicity. To test this visual impression of the data quantitatively, we randomly redistributed the x and y values of the 19 objects in Figure 2 (I_{CO} and $12 + \log(\text{O/H})$) 100,000 times. In only 97 of those 100,000 tests did all 8 detected objects in Figure 2 fall above an oxygen abundance of 7.9. The chance of obtaining the result randomly is only 0.1%, strongly suggesting that metal-poor dwarfs have markedly lower CO surface brightnesses.

EDITOR: PLACE FIGURE 2 HERE.

In previous works there has also been a clear trend for high metallicity galaxies to have a high CO emission, while most of the low abundance galaxies were undetected. Tacconi & Young (1985) noted a dependence of L_{CO} on metal abundance, although their sample of galaxies contained relatively massive, metal-rich objects and only 1 object with $12 + \log(\text{O/H}) < 8.5$. They presented a plot similar to our Figure 2, showing a clear correlation of L_{CO} with O/H for irregular and spiral galaxies, albeit with considerable scatter. Gondhalekar et al. (1998) also find a similar result. Part of this correlation was undoubtedly due to the underlying luminosity—metal abundance correlation among galaxies (*e.g.* Lequeux et al. 1979, Skillman, Kennicutt, & Hodge 1989). Arnault et al. (1988) made a similar plot using L_{CO}/M_{HI} , which shows a correlation between L_{CO}/M_{HI} and oxygen abundance. They include spiral galaxies while we specifically excluded spiral galaxies from our plot, both because the physical conditions of the molecular gas are likely to be different from dwarf galaxies, and because the concept of a global metal abundance is

ill-defined. Spiral galaxies often show large abundance gradients (e.g., Zaritsky, Kennicutt, & Huchra 1994), whereas dwarf and irregular galaxies have very uniform abundances (Pagel et al. 1980; Kobulnicky & Skillman 1996, 1997; Devost, Roy & Drissen 1997). Sage et al. (1992) present much the same plot (their Fig. 4a) from which they concluded that there is *no* correlation between L_{CO}/M_{HI} and metal abundance. Our restricted sample includes none of the Sage et al. galaxies, which are all more distant than 10 Mpc or more luminous than dwarf galaxies.

Figure 2 should be free from all of these biases due to differing distances, galaxy sizes, metallicities, and luminosities. We plot CO surface brightness rather than luminosity, and we include only dwarf galaxies which are chemically homogeneous. We also extend the metallicity baseline to much lower values of O/H in order to place stronger constraints on the role of metallicity in determining the CO surface brightness. Unfortunately, Figure 2 is relatively sparse because so few dwarf galaxies have sensitive CO observations and few of those have accurate metallicity determinations.

To increase the sample size using more of the galaxies from Table 3, we plot I_{CO} versus L_B in Figure 3. Given the metallicity – luminosity relationship for dwarf irregular galaxies, the luminosity can serve as a metallicity and size indicator. Mindful of the historical problems with false CO detections at low signal-to noise (e.g., Leo A) we further impose the restriction that the CO detection must be at the 4σ level or better. This excludes three objects, NGC 3738, DDO 83, and DDO 68, from Table 3. Labels and filled circles or large arrows denote galaxies with measured metallicities which appear in Figure 2. Filled triangles denote additional CO detections in objects without measured metallicities. Small arrows mark additional upper limits for galaxies which have been observed in CO. The addition of these 34 galaxies reinforces the striking trend seen in Figure 2. Galaxies detected in CO cluster near $\log I_{CO} = 0$ and have M_B brighter than -15.5 . No galaxies fainter than

$M_B = -15$ are detected, with the exception of the 4σ I Zw 36. Because I Zw 36 stands out in this way in Figures 2 and 3, it would be worthwhile to reobserve it for confirmation of the detection. The CO upper limits of the additional data from the literature do not constrain the behavior of I_{CO} at low metallicities as strongly as the new observations presented here.

EDITOR: PLACE FIGURE 3 HERE.

Since CO emission is considered a tracer of the molecular gas, it might be expected from the above result that low abundance galaxies would also be deficient in molecular gas compared to the amount of atomic gas. However, the conversion rate from CO to H_2 depends on abundance, in the sense that the lower the abundance, the higher the conversion rate. Therefore the low abundance galaxies will have the highest conversion rates (e.g., MB88), and thus may not necessarily have lower H_2 masses. The best evidence for a metallicity-dependent conversion factor dependent comes from CO observations of giant molecular clouds in metal poor systems in nearby galaxies (Verter & Hodge 1995, W95). The new, very sensitive data which we present here further strengthen their conclusions, and even suggest a rapid (non-linear) increase in X_{CO} below $12 + \log(O/H) = 8.0$. Spaans et al. (1998) find such a sharp change in X_{CO} at approximately this same metallicity in their models of the multi-phase galactic medium. Even more sensitive observations with the next generation of millimeter-wave telescopes may be able to confirm this prediction of a steep decline in CO surface brightness, and a steep increase in the I_{CO}/H_2 conversion factor in very metal-deficient environments.

5. Summary

^{12}CO $1 \rightarrow 0$ observations of 11 galaxies with oxygen abundances $12 + \log(O/H)$ in the range 8.4 to 7.3 yield the most sensitive data yet on very metal-deficient galaxies. The six

objects which have low abundances ($12+\log(\text{O/H}) < 8.0$) are not detected to upper limits of 0.1 K km s^{-1} . Three of these six have never before been observed in a CO line, while the others now have much more stringent upper limits. For the very low metallicity galaxy Leo A, we do not confirm a previously reported detection in CO, but the upper limit is consistent with an unpublished nondetection by L. Young (1997, private communication).

We combine these new observations with data from the literature to form a sample of dwarf galaxies which all have CO observations and measured oxygen abundances. None of the galaxies with $12+\log(\text{O/H}) < 7.9$ are detected. Most of the galaxies with higher metallicities are detected at a similar CO surface brightness, $\log I_{\text{CO}} \simeq -0.1 \text{ K km s}^{-1}$. These data are consistent with a strong dependence of the $I_{\text{CO}}/\text{M}_{\text{H}_2} \equiv X_{\text{CO}}$ conversion factor on ambient metallicity. The low upper limits on some galaxies, together with the molecular gas implied by the presence of star formation, are consistent with hypothesis that the conversion factor is non-linear, increasing sharply around 1/10 of the solar metallicity ($12+\log(\text{O/H}) \sim 8.0$).

We thank U. Klein for helpful comments on the paper, and C. Wilson for commenting on an earlier version of this paper. We thank the referee for a thorough review of the paper and useful comments. We are also grateful to the staff of NRAO-Tucson for their assistance with the observations. C. L. T. acknowledges support from the Deutsche Forschungsgemeinschaft under the framework of the Graduiertenkolleg “The Magellanic System and Other Dwarf Galaxies”. H. A. K. is grateful for assistance from a NASA Graduate Student Researchers Program fellowship and from #HF-01094.01-97A awarded by the Space Telescope Science Institute which is operated by the Association of Universities for Research in Astronomy, Inc. for NASA under contract NAS 5-26555. E. D. S. acknowledges support from NASA LTSARP Grant No. NAGW-3189.

REFERENCES

Aparicio, A., Garcia-Pelayo, J.M., Moles, M. 1988, *A&AS*, 74, 367 [AGM]

Arnault, P., Casoli, F., Combes, F. & Kunth, D. 1988, *A&A*, 205, 41 [Ae88]

Becker, R., Henkel, C., Bomans, D.J. & Wilson, T.L. 1995, *A&A*, 295, 302

Brinks, E. & Taylor, C.L. 1997, *IAU Symp.* 170 – Poster Proceedings, 12

Cohen, R.S., Dame, T.M., Garay, G., Montani, J., Rubio, M., & Thaddeus, P. 1988, *ApJ*, 331, L95

Devost, D., Roy, J.-R., & Drissen, L. 1997, *ApJ*, 482, 765

Dickman, R.L., Snell, R. L. & Schloerb, F.P. 1986, *ApJ*, 331, L95

Dohm-Palmer, R.C., Skillman, E.D., Saha, A., Tolstoy, E., Mateo, M., Gallagher, J., Hoessel, J., Chiosi, C. & Dufour, R.J. 1997, *AJ*, 114, 2514 [De97]

Elmegreen, B.G., Elmegreen, D.M., & Morris, M. 1980, *ApJ*, 240, 455 [Ee80]

Gallagher, J.S., Tolstoy, E., Dohm-Palmer, R.C., Skillman, E.D., Cole, A.A., Hoessel, J.G., Saha, A. & Mateo, M. 1998, *AJ*, 115, 1869 [Ge98]

Gondhalekar, P.M., Johansson, L.E.B., Brosch, N., Glass, I.S. & Brinks, E. 1998, *A&A*, 335, 152

Gonzalez-Delgado, R. M., et al. 1994, *ApJ*, 437, 239 [GDe94]

Greggio, L., Marconi, G., Tosi, M. & Focardi, P. 1993, *AJ* 105, 894 [Ge93]

Greve, A., Becker, R., Johansson, L.E.B. and McKeith, C.D. 1996, *A&A*, 312, 391

Hunter, D.A., Gallagher, J.S. & Rautenkranz, D. 1982, *ApJS*, 49, 53 [H82]

Hunter, D.A. & Sage, L.J. 1993, *PASP*, 105, 374 [HS93]

Israel, F.P. & Burton, W.B. 1986, *A&A*, 168, 369 [IB86]

Israel, F.P. & de Bruyn, A. G. 1988, *A&A*, 198, 115

Israel, F.P., De Graauw, Th., van de Stadt, H., & De Vries, C. P. 1986, *ApJ*, 303, 186

Israel, F.P., Johansson, L. E. B., Lequeux, J. et al. 1993, *A&A*, 276, 25 [Ie93]

Israel, F.P. & van Driel, 1990, *A&A*, 236, 323 [IvD]

Israel, F.P., Tacconi, L.J. & Baas, F. 1995, *A&A*, 295, 599 [Ie95]

Jackson, J.M., Snell, R.L., Ho, P.T.P. & Barrett, A.H. 1989, *ApJ*, 337 680

Kobulnicky et al. in preparation KeUP

Kobulnicky, H.A. & Skillman, E.D. 1995, *ApJ*, 454, L121 [KS95]

Kobulnicky, H.A. & Skillman, E.D. 1996, *ApJ*, 471, 211 [KS96]

Kobulnicky, H.A., & Skillman, E.D. 1997, *ApJ*, 489, 636 [KS97]

Kobulnicky, H.A., Skillman, E.D., Roy, J.-R., Walsh, J.R., Rosa, M.R. 1997, *ApJ*, 477, 679
[Ke97]

Lequeux, J., Peimbert, M., Rayo, J. F., Serrano, A., & Torres-Peimbert, S. 1979, *A&A*, 80, 155

Lo, K.Y., Sargent, W.L.W., & Young, K. 1993, *AJ*, 106, 507

Maloney, P. & Black, J.H. 1988, *ApJ*, 325, 389 [MB88]

Melisse, J.P.M. & Israel, F.P. 1994, *A&A*, 285, 51 [MI]

Morris, M. & Lo, K.Y. 1978, *ApJ*, 223, 803 [ML78]

Ohta, K., Tomita, A., Saito, M., Sasaki, M., & Nakai, N. 1993, *PASJ*, 45, L21

Pagel, B. E. J., Edmunds, M. G., Fosbury, R.A.E. & Webster, B.L. 1978, *MNRAS*, 184, 569

Pagel, B. E. J., Edmunds, M. G., & Smith, G. 1980, *MNRAS*, 193, 219

Patterson, R.J. & Thuan, T.X. 1996, *ApJS*, 107, 103 [PT]

Rogstad, D.H., Rougoor, G.W. & Whiteoak, J.B. 1967, *ApJ*, 150, 9

Rowan-Robinson, M., Phillips, T.G., & White, G. 1980, *A&A*, 82, 381 [RR80]

Rubio, M., Garay, G., Montani, J., & Thaddeus, P. 1991, *ApJ*, 368, 173

Rubio, M., Lequeux, J., & Boulanger, F. 1993, *A&A*, 271, 9

Sage, L.J., Salzer, J.J., Loose, H-H, & Henkel, C. 1992, *A&A*, 265, 19 [S92]

Salzer, J.J., MacAlpine, G.M. & Boroson, T.A. 1989, *ApJS*, 70, 447 [SMB]

Sanders, D. B., Scoville, N. Z., & Soifer, B. T. 1991, *ApJ*, 370, 158

Scoville, N.Z. & Sanders, D.B. 1987, in *Interstellar Processes*, eds. D.J. Hollenbach & H.A. Thronson (Dordrecht; Reidel), 21

Skillman, E.D., Bomans, D.J., & Kobulnicky, H. A. 1997, *ApJ*, 474, 205 [Se97]

Skillman, E.D., Kennicutt, R.C. & Hodge, P.W. 1989, *ApJ*, 347, 875 [SKH]

Skillman, E.D. & Kennicutt, R.C. 1993, *ApJ*, 411 655 [SK93]

Skillman, E.D., Terlevich, R.J., Kennicutt, R.C., Garnett, D.R., & Terlevich, E. 1994, *ApJ*, 431 172 [Se94]

Skillman, E.D., Terlevich, R., Teuben, P.J., & van Woerden, H. 1988, *A&A*, 198, 33 [Se88]

Spaans, M. 1998, et al. , 1998, in prep

Strong, A.W. et al. 1988, *A&A*, 207, 1

Tacconi, L.J. & Young, J.S. 1985, *ApJ*, 290, 602

Tacconi, L.J. & Young, J.S. 1987, *ApJ*, 322, 681

Talent, D. L. 1980, Ph.D. Thesis, Rice University [T80]

Taylor, C.L., Brinks, E., Grashuis, R.M. & Skillman, E.D. 1995, *ApJS*, 99, 427 [TBGS]

Terlevich, R., Melnick, J., Masegosa, J., Moles, M. & Copetti, M.V.F. 1991, *A&AS*, 91, 285 [Te95]

Thronson, H.A, & Bally, 1987, in *Star Formation in Galaxies*, ed. C.J. Lonsdale Persson (Washington:NASA), 267

Thronson, H.A., Hunter, D.A., Telesco, C.M., Greenhouse, M., & Harper, D.A. 1988, *ApJ*, 334, 605

Thuan, T.X. & Martin, G.E. 1981, *ApJ*, 247, 823 [TM81]

Tolstoy, E., Saha, A., Hoessel, J. G., & Danielson, G. E. 1995, *AJ*, 109, 579

Tolstoy, E. et al. 1998, *AJ*, in press [Te98]

Tully, B.R. 1988, *Nearby Galaxies Catalog*, 1988, Cambridge University Press: Cambridge. [T88]

Turner, J.L., Beck, S.C. & Hurt, R.L. 1997, *ApJ*, 474, L11

van Zee, L., Haynes, M.P. & Giovanelli, R. 1995, *AJ*, 109, 990 [vZ95]

van Zee, L., Haynes, M.P. & Salzer, J.J. 1997, *AJ*, 114, 2479 [vZ97]

Verter, F., & Hodge, P. 1995, *ApJ*, 446, 616 [VH95]

Viallefond, F., & Thuan, T. X. 1983, *ApJ*, 269, 444 [VT83]

Wiklind, T., & Henkel, C. 1989, *A&A*, 225, 1

Wilson, C.D. 1992, *ApJ*, 391, 144 [W92]

Wilson, C.D. 1995, *ApJ*, 448, L97

Young, J.S. et al. 1995, *ApJS*, 98, 219 [Ye95]

Young, J.S., Gallagher, J.H. & Hunter, D.A. 1984, *ApJ*, 276, 476

Young, L.M. & Lo, K.Y. 1996, *ApJ*, 462, 203

Zaritsky, D., Kennicutt, R.C. & Huchra, J.P. 1994, *ApJ*, 420, 87

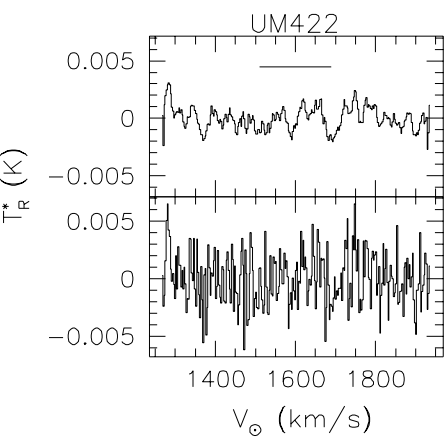
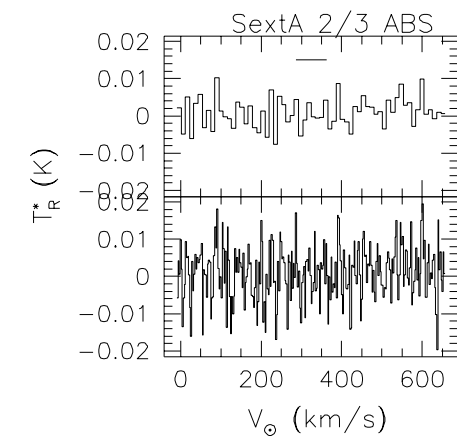
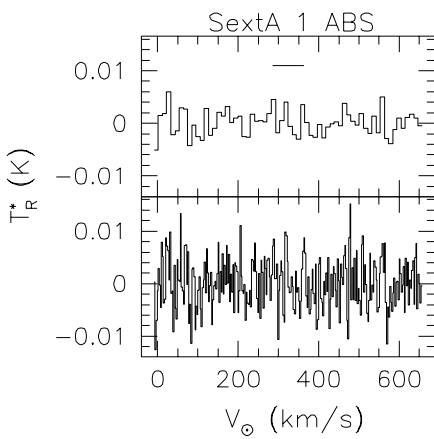
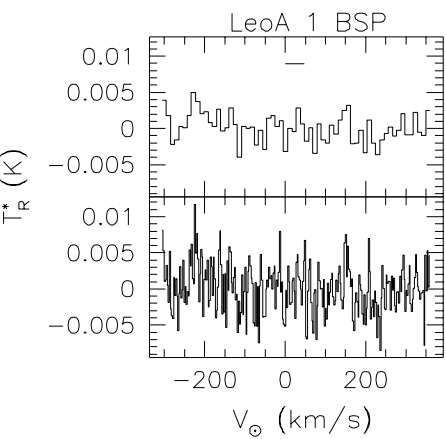
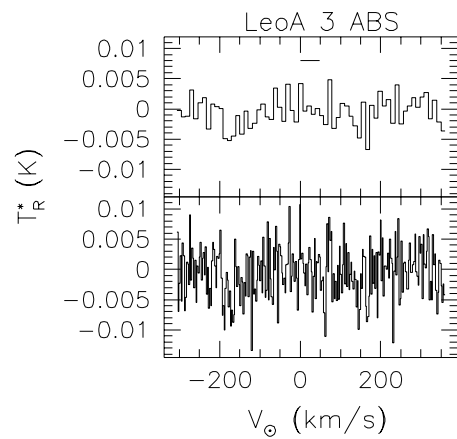
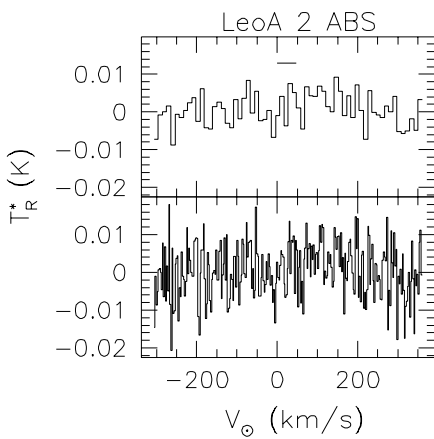
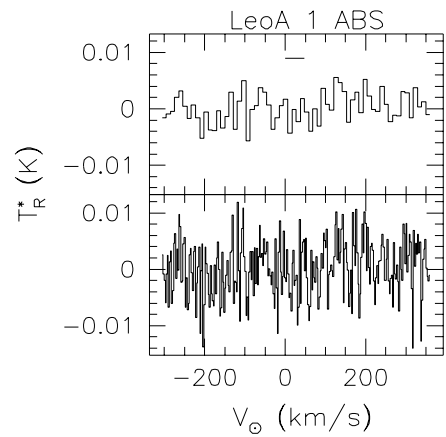
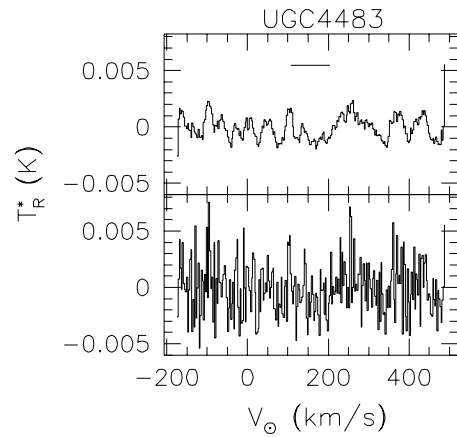
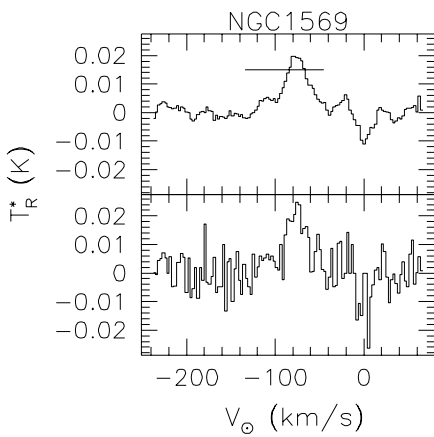
Figure Captions

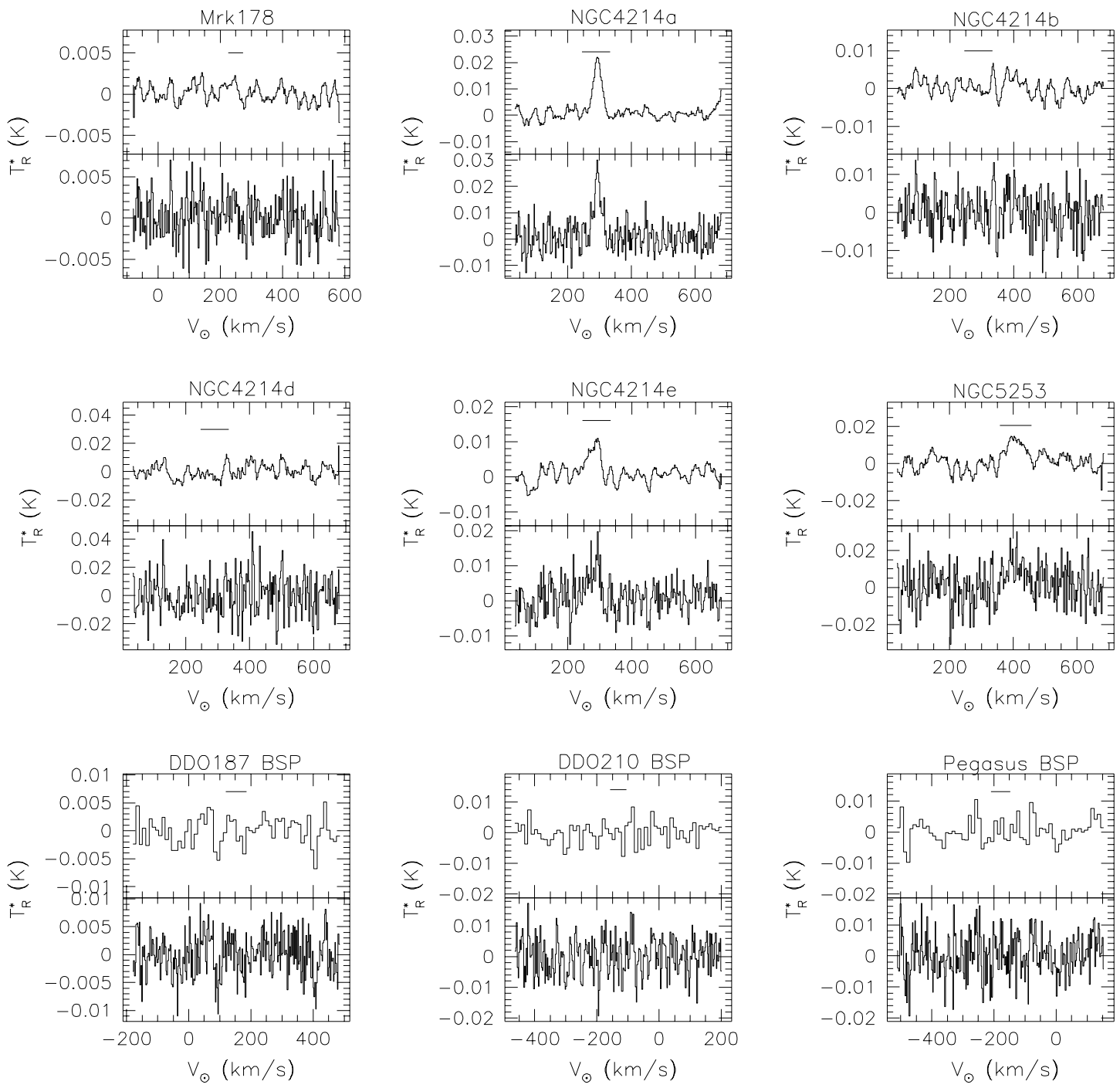
Fig. 1.— The spectra from the NRAO 12-m telescope. For each galaxy the upper spectrum is the original velocity resolution, 2.6 km s^{-1} , while the lower spectrum has been smoothed to 20 km s^{-1} . The horizontal line at the top of each plot shows the velocity position and full width at zero max of the HI profile for each galaxy. BPS indicates an observation in beam switching mode, ABS indicates absolute position switching. The galaxies shown are the following: NGC 1569, UGC 4483, Leo A, Sextans A, UM422, Mrk 178, NGC 4214, NGC 5253, DDO 187, DDO 210, and Pegasus.

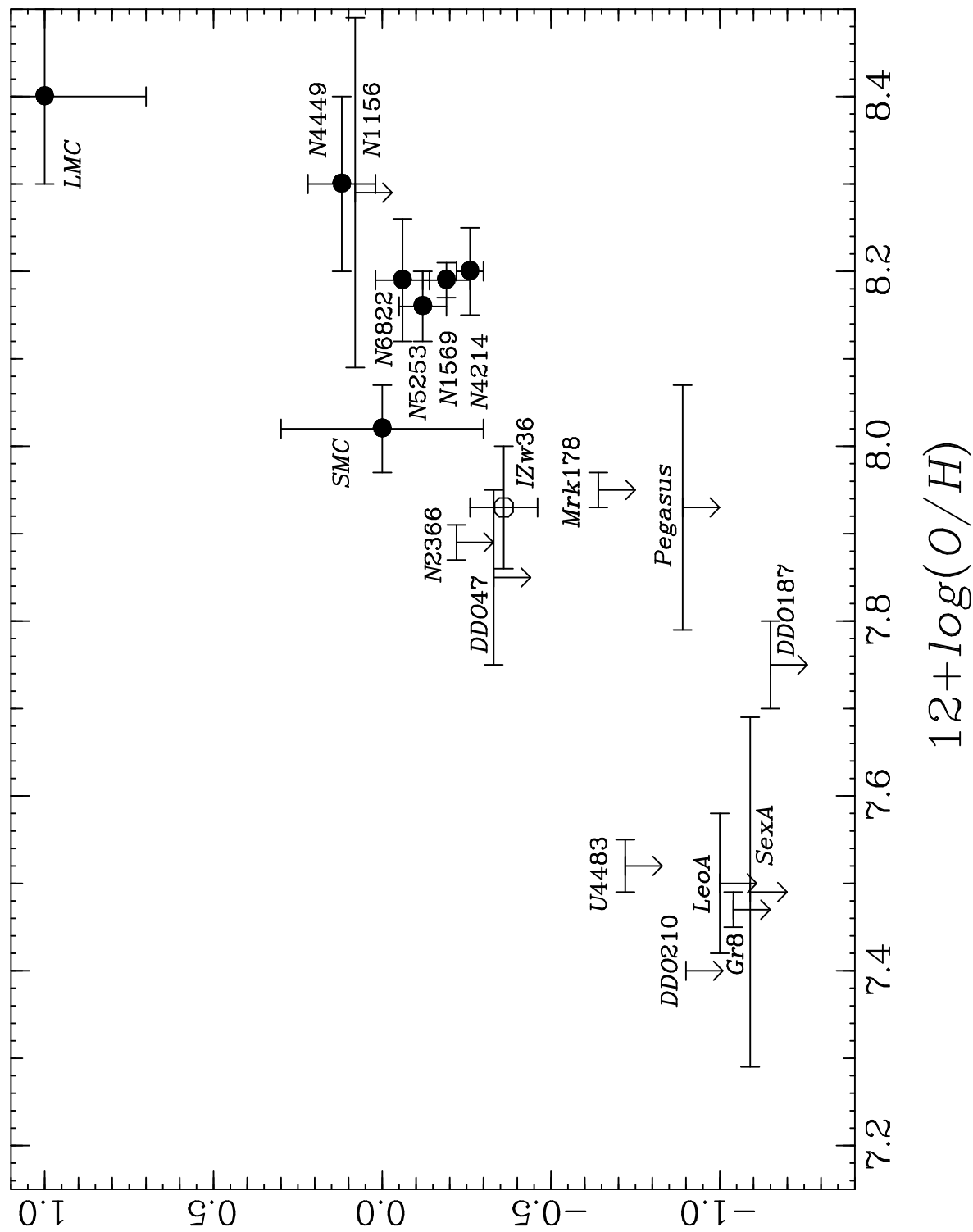
Fig. 2.— $\log (I_{CO})$ versus oxygen abundance, $12 + \log(O/H)$, for all known dwarf ($M > -18$) galaxies within 10 Mpc which have CO observations and measured oxygen abundances. Filled circles denote $> 4\sigma$ detections. Positions of the SMC and LMC are mean values reported by Israel et al. (1993). For NGC 4214 and NGC 6822, only the locations of the peak CO surface brightness are plotted. The open circle represents a marginal (4σ) detection of I Zw 36 that has not been confirmed. All other systems have only upper limits, including some very low limits on extremely metal-poor systems reported in this work. It is striking that no galaxies with $12 + \log(O/H) < 7.9$ ($Z < 0.1 Z_{\odot}$) have been detected in CO, indicating that extremely metal-poor systems have much lower mean CO surface brightnesses. This data is consistent with a rise (perhaps sharply non-linear) in the $I_{CO}/M_{H_2} \equiv X_{CO}$ conversion factor at metallicities below 0.1 of the solar value.

Fig. 3.— $\log (I_{CO})$ versus absolute blue magnitude, M_B , for dwarf ($M > -18$) galaxies within 10 Mpc which have CO observations. A few objects with reported detections at less than the 4σ level appear as upper limits instead (see text). We plot objects from Figure 2 using the same filled circles and downward arrows. Thirty-four additional objects with measured magnitudes but without measured oxygen abundances appear on this plot compared to Figure 2. Filled triangles denote the four additional detections, while smaller

arrows without seraphs show the 30 non-detections. This diagram is consistent with the clear lack of CO detections at very low metallicities seen in Figure 2. However, the upper limits on these additional data are not especially helpful at constraining the relationship between CO surface brightness and metallicity.







$$12 + \log(O/H)$$

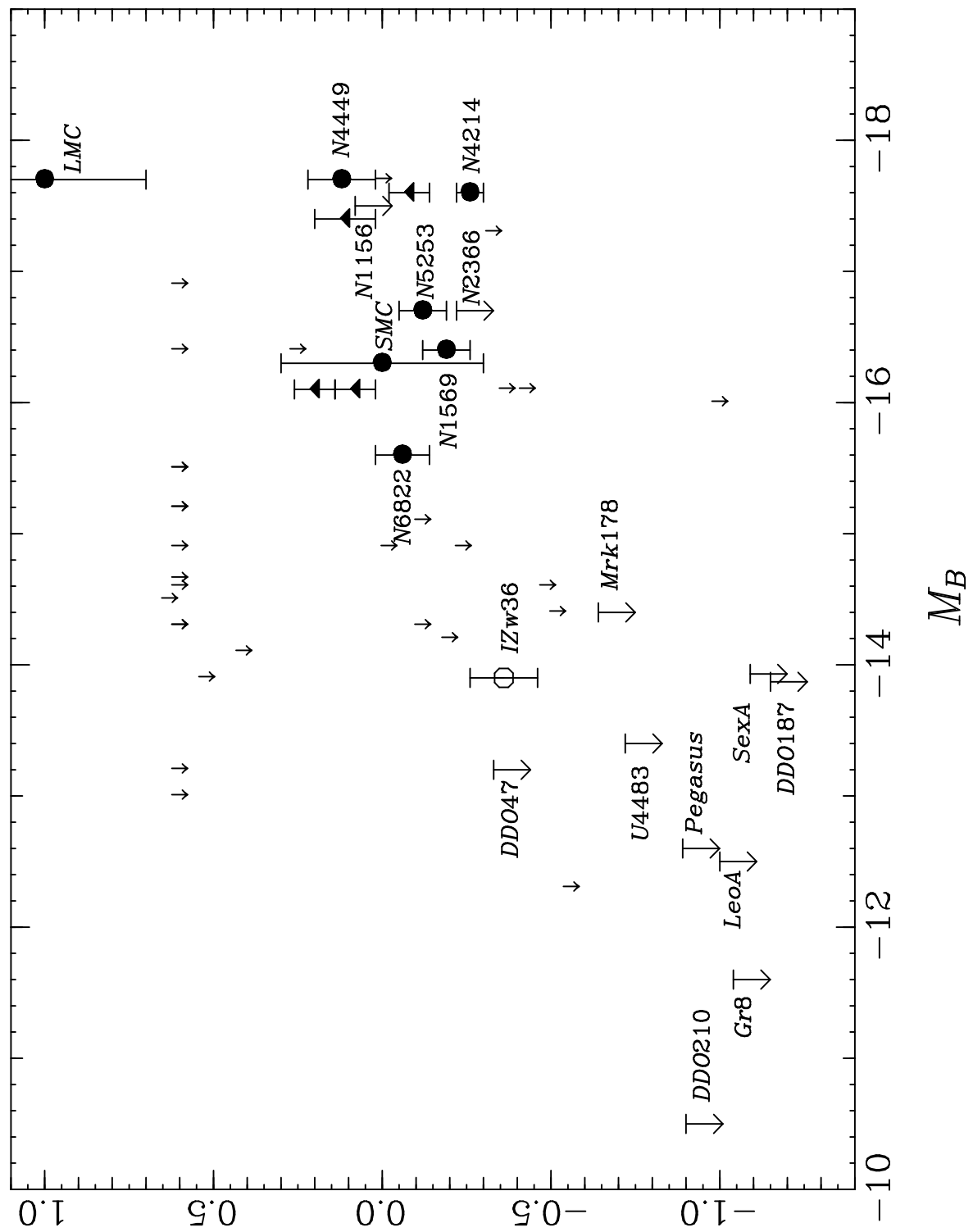


Table 1. Velocities and Linewidths

Galaxy Name	α (1950)	δ (1950)	D_{25} '	$v_{\odot}(\text{HI})$ (km s $^{-1}$)	$\Delta v_{50}(\text{HI})$ (km s $^{-1}$)	HI Reference	$v_{\odot}(\text{CO})$ (km s $^{-1}$)	$\Delta v_{50}(\text{CO})$ (km s $^{-1}$)	$\sigma(T_R^*)$ (K)	$I(\text{CO})$ (K km s $^{-1}$)
NGC 1569	04:26:05	+64:44:23	3.1	-89	74	[H82]	-76	29	0.007	0.685 ± 0.007
UGC 4483	08:32:07	+69:57:16	1.1	156	49	[MI]	0.002	< 0.19
Leo A	5.0	20	33	[MI]
Leo A-1(ABS)	09:56:38	+30:58:50	0.004	< 0.12
Leo A-2	09:56:21	+30:59:29	0.006	< 0.12
Leo A-3	09:56:32	+30:59:12	0.004	< 0.08
Leo A-1(BPS)	09:56:38	+30:58:50	0.003	< 0.08
Sextans	4.4	325	46	[Se88]
Sextans A-1	10:08:36	-04:27:34	0.004	< 0.08
Sextans A-2	10:08:32	-04:27:34	0.006	< 0.12
Sextans A-3	10:08:21	-04:26:40	0.006	< 0.12
UM422	11:17:40	+02:47:58	2.3	1600	90	[TBGS]	0.002	< 0.12
Mrk 178	11:30:45	+49:30:46	1.4	250	30	[TM81]	0.002	< 0.22
NGC 4214	9.6	290	62	[MI]	0.900 \pm 0.000
NGC 4214a	12:13:09	+36:36:16	294	26	0.005	0.542 \pm 0.000
NGC 4214b	12:13:11	+36:35:44	0.005	< 0.08
NGC 4214d	12:13:11	+36:36:48	0.013	< 0.08
NGC 4214e	12:13:06	+36:36:48	282	40	0.004	0.358 \pm 0.000
NGC 5253	13:37:05	-31:23:30	4.5	408	60	[KS95]	400	60	0.009	0.725 \pm 0.000
DDO 187	14:13:38	+23:17:10	1.9	154	33	[MI]	0.003	< 0.07
DDO 210	20:44:06	-13:01:55	2.3	-137	21	[MI]	0.005	< 0.12
Pegasus	23:26:04	+14:27:15	4.6	-183	23	[MI]	0.005	< 0.13

Table 2. Properties of Observed Dwarf Galaxies

Galaxy Name	Galaxy Name	Distance (Mpc)	Reference	M_B	Reference	Abundance $12 + \log \text{O/H}$	Reference	I_{CO} (K km s $^{-1}$)	L_{CO} (10^6 K km/s pc 2)
NGC 1569	VII Zw 16	2.2	[IvD]	-16.9	[T88]	8.19 ± 0.02	[KS97]	0.685 ± 0.104	0.18 ± 0.03
NGC 4214	UGC 7278	4.1	[MI]	-17.9	[T88]	8.20 ± 0.05	[KS96]	0.900 ± 0.105	0.91 ± 0.12
NGC 5253	UGCA 369	4.1	[KS95]	-17.2	[T88]	8.20 ± 0.06	[Ke97]	0.725 ± 0.148	0.68 ± 0.14
UM422	UGC 6345B	21.3	[TBGS]	-13.7	[SMB]	8.0 ± 0.2	[Te95]	< 0.120	< 3.0
Mrk 178	UGC 6541	4.2	[TM81]	-14.4	[T88]	8.0 ± 0.02	[KS96]	< 0.225	< 0.22
Pegasus	DDO 216	0.76	[Ge98]	-12.3	[T88]	7.93 ± 0.11	[Se97]	< 0.0044	< 0.132
UGC 4483	...	4.0	[MI]	-13.4	[MI]	7.50 ± 0.03	[Se94]	< 0.195	< 0.18
Sextans A	DDO 75	1.4	[De97]	-14.1	[T88]	7.5 ± 0.2	[SKH]	< 0.017	< 0.143
DDO 210	...	4	[Ge93]	-13.4	[MI]	7.4 ± 1.3	...	< 0.11	< 0.125
DDO 187	UGC 9128	4.4	[AGM]	-13.9	[T88]	7.75 ± 0.05	[vZ97]	< 0.076	< 0.070
Leo A	DDO 69	0.69	[Te98]	-11.7	[T88]	7.3 ± 0.2	[SKH]	< 0.0037	< 0.143

References for Table 2.

a) estimated from the magnitude/abundance relation from Skillman *et al.* (1989);

Table 3. Data for Galaxies in the Literature

Galaxy Name	Galaxy Name	Distance (Mpc)	Reference	M_B	Reference	Abundance 12 + log O/H	Reference	I_{CO} (K km s $^{-1}$)	Reference	L_{CO} (10 6 K km s $^{-1}$)
NGC1156	VV531	6.4	[T88]	-17.5	[T88]	8.29(0.20)	[T80]	<1.2	[HS93]	<2.0
UGCA372	Mrk67	22.4	[T88]	-16.0	[TM81]	8.21(0.08)	[KS96]	<0.62	[S92]	<2.0
NGC6822	DDO 209	0.7	[T88]	-15.6	[T88]	8.19(0.07)	[KS96]	>1.81(0.25)	[W92]	0.05 (0.0)
IIZw40	UGCA116	10.3	[T88]	-17.2	[T88]	8.06(0.02)	[KeUP]	0.46(0.10)	[Ye95]	1.82 (0.0)
IIZw70	Mrk829	23.1	[T88]	-17.1	[T88]	8.06(0.08)	[KS96]	<0.38	[Ye95]	<7.0
UM439	UGC06578	14.7	[vZ95]	-15.8	[SMB]	8.05(0.02)	[KS95]	<0.48	[S92]	<5.7
IIZw123	Mrk487	15.0	[T88]	-16.1	[T88]	8.02(0.09)	[KS96]	<1.06	[Ae88]	<2.1
SMC	...	0.06	[BW97]	-16.3	[BT88]	7.98(0.02)	[Pe78]	1.0(0.5)	[Ie93]	5200(200)
UM462	Mrk1307	13.9	[TBGS]	-15.7	[S92]	7.96(0.02)	[KS96]	<0.28	[BT]	<3.0
IIZw36	UGCA281	4.7	[T88]	-13.9	[T88]	7.93(0.07)	[VT83]	0.45(0.10)	[Ye95]	0.37 (0.0)
NGC2366	DDO 42	2.9	[T88]	-16.7	[T88]	7.89(0.02)	[GDe94]	<0.60	[HS93]	<0.2
UGC3974	DDO 47	2.1	[T88]	-13.2	[T88]	7.85(0.01)	[SKH]	<0.46	[Ye95]	<0.0
UM461	...	11.7	[S92]	-14.1	[S92]	7.76(0.02)	[KS96]	<0.78	[S92]	<5.9
NGC4789A	DDO 154	4.0	[T88]	-14.1	[T88]	7.67(0.06)	[vZ97]	<2.6	[ML78]	<2.3
GR8	DDO 155	1.7	[T88]	-11.6	[T88]	7.47(0.02)	[SKH]	<0.09	[VH95]	<0.0
IIZw18	Mrk116	14.3	[T88]	-14.8	[TM81]	7.21(0.05)	[SK93]	<0.27	[Ge98]	<1.2
Arp4	DDO 14	19.8	[T88]	-17.9	[T88]	<1.38	[IB86]	<30.0
NGC3353	Haro3	16.8	[T88]	-17.9	[T88]	1.46(0.21)	[S92]	3.68 0
UM549	...	78.7	[SMB]	-17.9	[SMB]	<0.27	[Ge98]	<37.0
UGC12632	DDO 217	9.2	[T88]	-17.7	[T88]	<0.99	[IB86]	<4.0
NGC2537	Mrk86	9.0	[T88]	-17.6	[T88]	0.83(0.12)	[S92]	0.60(0.0)
UGC10310	DDO 204	15.8	[T88]	-17.5	[T88]	<3.2	[ML78]	<44.0

Table 3. (continued)

Galaxy Name	Galaxy Name	Distance (Mpc)	Reference	M_B	Reference	Abundance 12 + log O/H	Reference	I_{CO} (K km s $^{-1}$)	Reference	L_{CO} (10 6 K km s $^{-1}$)
UM471	...	146.6	[SMB]	-17.5	[SMB]	<0.46	[Ge98]	< 22
NGC4605	UGC07831	4.0	[T88]	-17.4	[T88]	1.3(0.3)	[TB87]	3.39(0)
HoII	DDO 50	4.5	[T88]	-17.3	[T88]	<0.46	[Ye95]	< 0.1
UM465	UGC6877	15.4	[T88]	-17.3	[T88]	0.63(0.18)	[S92]	8.34(2)
UGC05478	DDO 73	23.4	[T88]	-17.2	[T88]	<0.30	[Ie95]	<9.1
NGC4670	Haro9	11.0	[T88]	-17.2	[T88]	<2.62	[Ae88]	<2.8
UM286	...	21.6	[T88]	-17.0	[T88]	<0.73	[Ge98]	<7.7
UM334	...	69.5	[SMB]	-17.0	[SMB]	<0.36	[Ge98]	<39
UM454	...	50.1	[SMB]	-17.0	[SMB]	<0.73	[Ge98]	<41
NGC4144	UGC7151	4.1	[T88]	-16.9	[T88]	<4.0	[RR80]	<3.7
UM351	...	104.2	[SMB]	-16.9	[SMB]	<0.27	[Ge98]	<66
NGC4523	DDO 135	16.8	[T88]	-16.8	[T88]	<0.57	[Ye95]	<6.0
UM374	...	79.1	[SMB]	-16.8	[SMB]	<0.46	[Ge98]	< 65
NGC7077	Mrk900	13.3	[T88]	-16.7	[T88]	0.50(0.09)	[S92]	0.79(0)
UGCA441	Mrk328	19.6	[T88]	-16.6	[T88]	<1.04	[S92]	<3.5
UM483	Mrk1313	30.8	[TBGS]	-16.5	[SMB]	<0.73	[Ge98]	<15
IC2574	DDO 81	2.7	[T88]	-16.4	[T88]	<1.8	[Ee80]	<0.7
NGC1560	UGC03060	3.0	[T88]	-16.4	[T88]	<4.0	[RR80]	<2.0
UM491	...	26.3	[TBGS]	-16.3	[SMB]	<0.73	[Ge98]	<11
UM456	...	23.3	[TBGS]	-16.1	[S92]	<0.64	[Ge98]	<7.8
NGC4707	DDO 150	8.0	[T88]	-16.1	[T88]	<0.42	[Ie95]	<1.5
NGC3077	UGC05398	2.1	[T88]	-16.1	[T88]	1.59(0.26)	[Ye95]	0.26(0)
NGC3738	UGC06565	4.3	[T88]	-16.1	[T88]	0.37(0.10)	[Ye95]	0.26(0)
NGC2976	UGC05221	2.1	[T88]	-16.1	[T88]	1.2(0.2)	[TB87]	0.86(0)
NGC3274	UGC05721	5.9	[T88]	-16.0	[T88]	< 0.1	[TB87]	< 0
UM323	...	25.5	[TBGS]	-15.9	[SMB]	<0.55	[Ge98]	<8.0
UM452	...	19.2	[TBGS]	-15.9	[SMB]	<0.64	[Ge98]	<5.3

Table 3. (continued)

Galaxy Name	Galaxy Name	Distance (Mpc)	Reference	M_B	Reference	Abundance 12 + log O/H	Reference	I_{CO} (K km s $^{-1}$)	Reference	L_{CO} (10 6 K km s $^{-1}$)
UGC03966	DDO 46	7.4	[T88]	-15.5	[T88]	<4.0	[RR80]	<12
UGC08320	DDO 168	3.6	[T88]	-15.5	[T88]	<4.0	[RR80]	<2.8
UM533	UGC08105	10.4	[S92]	-15.3	[S92]	<0.87	[S92]	<5.2
UGC09405	DDO194	5.7	[T88]	-15.2	[MI]	<4.0	[RR80]	<7.2
HoI	DDO 63	4.4	[T88]	-15.2	[T88]	<4.0	[RR80]	<4.3
UGC05272	DDO 64	6.5	[T88]	-15.1	[T88]	<0.75	[Ie95]	<1.7
UGC02014	DDO 22	9.9	[T88]	-14.9	[MI]	<0.95	[IB86]	<5.2
UGC05764	DDO 83	6.9	[T88]	-14.9	[T88]	0.57(0.20)	[Ie95]	1.52(0)
UGC07698	DDO 133	3.8	[T88]	-14.9	[T88]	<4.0	[RR80]	<3.2
UGC03860	DDO 43	7.2	[T88]	-14.6	[T88]	<0.32	[Ie95]	<0.9
UGC07577	DDO 125	3.0	[T88]	-14.6	[T88]	<4.0	[RR80]	<2.0
VII Zw499	DDO 165	2.8	[T88]	-14.6	[T88]	<4.0	[RR80]	<1.7
IZw87	DDO 190	3.7	[T88]	-14.5	[T88]	<0.46	[Ie95]	<0.3
UGC05340	DDO 68	5.9	[T88]	-14.4	[T88]	0.30(0.15)	[Ie95]	0.58(0)
UGC06817	DDO 99	3.1	[T88]	-14.3	[T88]	<4.0	[RR80]	<2.1
IC1574	DDO 226	4.5	[T88]	-14.3	[T88]	<4.0	[RR80]	<4.5
UGC06900	DDO 101	5.9	[T88]	-14.3	[T88]	<0.75	[Ie95]	<1.4
UGC04426	DDO 52	6.3	[T88]	-14.2	[T88]	<0.63	[Ie95]	<1.4
UGC08760	DDO 183	3.3	[T88]	-13.9	[T88]	<0.30	[Ie95]	<0.1
UGC07559	DDO 126	2.8	[T88]	-13.2	[T88]	<4.0	[RR80]	<1.7
UGC07599	DDO 127	3.5	[T88]	-13.0	[T88]	<4.0	[RR80]	<2.7
M81DwA	...	4.3	[T88]	-12.3	[PT]	<0.27	[Ye95]	<0.1